

HEPATOLOGY

Hepatic autophagy mediates ER stress-induced degradation of misfolded apolipoprotein B

Journal:	<i>Hepatology</i>
Manuscript ID:	HEP-10-1546
Wiley - Manuscript type:	Original
Date Submitted by the Author:	07-Sep-2010
Complete List of Authors:	Qiu, Wei; Hospital for Sick Children Zhang, Jing; Hospital for Sick Children Dekker, Mark; Hospital for Sick Children Wang, Huajin; Hospital for Sick Children Huang, Ju; Hospital for Sick Children Adeli, Khosrow; The Hospital for Sick Children, Division of Biochemistsry, DPLM Brumell, John; Hospital for Sick Children
Keywords:	Hepatocytes, Autophagy, Apolipoprotein B, ER stress, Degradation

SCHOLARONE™
Manuscripts

1
2
3 **Hepatic autophagy mediates ER stress-induced degradation of misfolded apolipoprotein B**

4
5
6
7 Wei Qiu,¹ Jing Zhang,¹ Mark J Dekker,¹ Huajin Wang,¹ Ju Huang,² John H Brumell,² and
8 Khosrow Adeli^{1*}
9

10
11 ¹Molecular Structure & Function and ² Cell Biology Programs, Research Institute, The Hospital
12 for Sick Children, University of Toronto, Ontario, M5G 1X8, Canada
13
14

15 Running title: ER stress-induced apoB autophagy
16
17
18
19
20
21
22
23
24
25 *To whom correspondence should be addressed:
26
27
28
29
30
31
32
33
34
35
36
37
38
39
40
41
42
43
44
45
46
47
48
49
50
51
52
53
54
55
56
57
58
59
60

Khosrow Adeli
Division of Clinical Biochemistry, DPLM
Hospital for Sick Children
University of Toronto
Toronto, Ontario, Canada
M5G 1X8
Phone: 416-813-8682
Fax: 416-813-6257
E-mail: k.adeli@utoronto.ca

Abbreviations used are: apoB, apolipoprotein B; ALLN, N-acetyl-leucinyl-leucinyl-norleucinal; ATF, activating transcription factor; eIF α , α -subunit of eukaryotic translational initiation factor 2; ER, endoplasmic reticulum; GFP, green fluorescent protein; GLS, glucosamine; IRE1, inositol requirement 1; LC3, microtubule associated protein1 light chain 3; PAGE, polyacrylamide gel electrophoresis; PBA, 4-Phenyl butyric acid; PBS, phosphate-buffered saline; PERK, PKR-like endoplasmic reticulum kinase; PERPP, post-ER pre-secretory proteolysis pathway; SDS, sodium dodecyl sulfate; TG, triglyceride; TM, tunicamycin; VLDL, very low density lipoprotein; Xbp1, x-box binding protein 1.

Abstract:

Induction of ER stress was previously shown to impair hepatic apoB100 production by enhancing co- and post-translational degradation of apoB. Here, we report the involvement of autophagy in ER stress-induced degradation of apoB and provide evidence for a significant role of autophagy in regulating apoB biogenesis in primary hepatocyte systems. Induction of ER stress following short-term glucosamine treatment of McA-RH7777 cells resulted in significantly increased co-localization of apoB with GFP-LC3, referred to as apoB-GFP-LC3 puncta, in a dose-dependent manner. Co-localization with this autophagic marker correlated positively with the reduction in newly-synthesized apoB100. Treatment of McA-RH7777 cells with 4-Phenyl butyric acid (PBA), a chemical ER stress inhibitor, prevented glucosamine and tunicamycin-induced increases in GRP78 and phosphorylated eIF2 α , rescued newly-synthesized [35 S] labelled apoB100, and substantially blocked the co-localization of apoB with GFP-LC3. Autophagic apoB degradation was also observed in primary rat and hamster hepatocytes at basal as well as upon the induction of ER stress. In contrast, this pathway was inactive in HepG2 cells under ER stress conditions, unless proteasomal degradation was blocked with ALLN and the medium was supplemented with oleate. Transient transfection of McA-RH7777 cells with a wild type PKR-like ER kinase cDNA resulted in dramatic induction of apoB autophagy. In contrast, transfection with a kinase inactive mutant PERK gave rise to reduced apoB autophagy, suggesting that apoB autophagy may occur *via* a PERK signalling-dependent mechanism. Taken together, these data suggest that induction of ER stress leads to markedly enhanced apoB autophagy in a PERK dependent pathway, that can be blocked with a chemical chaperone, PBA. ApoB autophagy rather than proteasomal degradation may be a more physiological mechanism regulating hepatic lipoprotein production in primary hepatocytes.

Introduction

Apolipoprotein B100 (apoB), the major protein component of LDL and VLDL, is constitutively synthesized in the liver and regulated through co- and post-translational degradation(1;2). Intracellular degradation of newly-synthesized apoB has been shown to involve various mechanisms including ERAD (Endoplasmic reticulum (ER)-associated degradation), ER60-associated degradation, LDL receptor-associated degradation and autophagy. ERAD, an early-stage protein quality control system, is the most extensively studied apoB degradation pathway in cell culture models such as the HepG2 human hepatoma cell line (3;4). In lipid poor conditions or in the absence of microsomal triglyceride transfer protein (MTP) activity, a large proportion of newly-synthesized apoB is rapidly ubiquitinated and degraded by the proteasome(5). ERAD has also been implicated in apoB degradation in primary hepatocytes which were shown to ubiquitinate and degrade apoB *via* the proteasome, although at much lower rate compared to HepG2 cells (6). Experimental evidence has also suggested that N-terminal cleavage of nascent apoB is another mechanism involved in the proteolysis of apoB within the ER lumen. Using a permeabilized cell system, we reported the existence of a nonproteasomal degradative pathway that is responsible for specific fragmentation of apoB and generation of a 70 kDa fragment (7). Permeabilized cells, largely devoid of the cytosolic proteasome components, continued to degrade apoB and generated specific fragments, including a 70 kDa fragment, *via* a lactacystin insensitive process(8). This observation was supported by Du et al. who demonstrated that an N-terminal of 85KDa-apoB fragment was generated in microsomes following transient overexpression of human apoB53 in CHO cells (9). Studies with LDL receptor deficient hepatocytes ($Ldlr^{-/-}$) have revealed that LDL receptor plays a critical role in the degradation of newly-synthesized apoB (10). Twisk et al. reported that LDL receptor

1
2
3 deficient hepatocytes ($Ldlr^{-/-}$) secreted more apoB100 as compared to wild-type hepatocytes
4 due to reduced degradation of newly-synthesized apoB in $Ldlr^{-/-}$ hepatocytes. Recently, more
5 evidence has been obtained showing that apoB turnover is associated with the levels of the LDL
6 receptor. Proprotein convertase subtilisin/kexin type 9 (PCSK9), predominantly expressed in
7 liver, was found to increase secretion of apoB *via* downregulation of hepatic LDL receptor
8 protein (11).
9
10

11 Growing evidence also suggests that autophagy, a late-stage protein quality control
12 system, can mediate apoB degradation (12-14). Autophagy is a degradation process for cellular
13 components in which double-membrane autophagosomes sequester organelles or portions of
14 cytosol and fuse with lysosomes or vacuoles to facilitate breakdown by resident hydrolases(15).
15 Ohsaki et al. first observed that apoB degradation was associated with the lipid droplet (LD) in
16 the cytoplasm through an autophagic mechanism(12). Soon after, Pan et al. showed that
17 autophagic degradation of apoB occurred *via* post-ER presecretory proteolysis (PERPP), induced
18 by reactive oxygen species (ROS) generated within hepatocytes from dietary polyunsaturated
19 fatty acids (PUFA) (13). More recently, Yao and colleagues demonstrated autophagic
20 degradation of an apoB mutant (A31P), which led to decreased secretion of endogenous apoB
21 and triglycerides (14). Thus ample evidence now exists for apoB autophagy, although the
22 molecular mechanisms involved in targeting apoB to intracellular autophagy are currently
23 unknown.
24
25

26 Available evidence indicates that ER stress induced by misfolded or malfolded proteins
27 may trigger insulin resistance, dyslipidemia, and diabetes (16). We previously reported that
28 induction of ER stress (with glucosamine treatment) leads to misfolding of newly-synthesized
29 apoB in the ER and the elimination of apoB *via* proteasomal and non-proteasomal
30
31
32
33
34
35
36
37
38
39
40
41
42
43
44
45
46
47
48
49
50
51
52
53
54
55
56
57
58
59
60

1
2
3 mechanisms(17). ApoB100 stability showed a strong inverse correlation with the expression of
4 glucose regulated protein 78 (GRP78), a key marker of ER stress(17). GRP78 overexpression
5 induced rapid degradation of newly-synthesized apoB100 (17). In line with these observations,
6 Ginsberg and colleagues showed that treatment of McARH7777 cells with oleate at a high
7 concentration (1.2 mM) or for a long period of time (16 hours) induced ER stress and
8 upregulated GRP78 (18). Interestingly, GRP78 has been implicated in not only ERAD induction
9 but also stress-induced autophagy (19).

10
11 In the current report, we present evidence implicating autophagy in ER stress induced
12 degradation of misfolded apoB. Under ER stress, apoB autophagy appears to be PERK
13 dependent and is more pronounced in primary hepatocytes compared to established cell lines.
14 Our data suggest that autophagy may be a physiologically-important mechanism for the
15 degradation of misfolded apoB under ER stress conditions.

Materials and Methods

Cell culture and transient transfection. McA-RH7777 and HepG2 cells were purchased from ATCC (Manassas, VA). The cells were maintained in Dulbecco's modified Eagle's medium (DMEM) (Life Technologies, Inc.) containing 20 % or 10 % fetal calf serum, respectively. Isolation of primary hepatocytes from rat or hamster was described previously (20). The cells (5×10^5) were seeded in 6-well plates 4 hours before the experiments. 1 μ g of GFP-LC3 cDNA (21) alone or and 1 μ g of wild-type (WT) PERK cDNA or kinase inactive mutant PERK (MPERK) cDNA (22) were co-transfected into the cells using Lipofectamine 2000 (Life Technologies, Grand Island, NY) according to the manufacturer's protocol.

Immunoblot analysis. Following treatment with 5 mM glucosamine (GLS), or 5 μ g/ml tunicamycin (TM), cultured cells were washed twice with PBS and lysed using solubilizing buffer (PBS containing 1% Nonidet P-40, 1% deoxycholate, 5 mM EDTA, 1 mM EGTA, 1 mM PMSF, 100 kallikrein-inactivating units/ml aprotinin, and phosphatase inhibitors as described previously) (23). The membranes were blocked with a solution of 1% of BSA, incubated with the indicated antibodies (see figure legends), and then incubated with appropriate secondary antibodies conjugated to horseradish peroxidise (HRP). Monoclonal anti-KDEL antibody was from CalBiochem (San Diego, CA). Anti-phosphorylated-eIF2 α , and anti-eIF2 α antibodies were from Oncogene (Boston, MA). Rabbit polyclonal anti-LC3 was from Novus Biologicals, Inc (Littleton, CO).

Metabolic labelling, Immunoprecipitation, SDS-PAGE, and fluorography. After a 2-hour treatment of McA-RH7777 cells or primary rat hepatocytes with 5 mM glucosamine or 5 μ g/ml tunicamycin, the cells were preincubated in methionine/cysteine-free MEM with 5 mM glucosamine or 5 μ g/ml tunicamycin at 37 °C for 1 hour, followed by pulse-labeling with 100

1
2
3 $\mu\text{Ci}/\text{ml}$ [^{35}S] methionine for 2 hours in the presence or absence of 1mM PBA (see figure
4 legends). Following the pulse, the medium was harvested for immunoprecipitation of secreted
5 apoB100 or albumin. The cells were lysed using 500 μl solubilizing buffer and cellular apoB100
6 was immunoprecipitated under the conditions described in the figure legends. The gels were
7 fixed and saturated with Amplify (Amersham Pharmacia Biotech) before being dried and
8 exposed to Kodak Hyperfilm at -80 °C for 1–4 days. Films were developed and quantitative
9 analysis of apoB100 bands was performed using an imaging densitometer (24).
10
11

12 **RT-PCR analysis of mRNA.** Following treatment of McA-RH7777 cells with 5 mM
13 glucosamine or 5 $\mu\text{g}/\text{ml}$ tunicamycin for 4 hours in the presence or absence of 1mM PBA, total
14 RNA was extracted using a commercially available kit (RNeasy; Qiagen). First-strand cDNA
15 was synthesized from 5 μg of total RNA using SuperScript II reverse transcriptase
16 (Invitrogen)(25). The resulting cDNA was subjected to 28 cycles of PCR amplification
17 (denaturation at 95°C for 30s; annealing at 55°C for 60s; extension at 72°C for 90s). The primer
18 pairs used for detecting mRNA levels are listed in supplemental data 1.
19
20

21 **Immunofluorescence Microscopy.** Following 24-48 hours transfection, cells were fixed with
22 pre-cooled 100% methanol for 5 minutes and then permeabilized with 0.1% Triton X100 in PBS
23 for 4 minutes. Cells were incubated with rabbit anti-hamster apoB antibody (1:1000) for 1 hour
24 at room temperature or overnight at 4°C in 5% BSA. Secondary antibody used in this study was
25 CyTM3-conjugated affiniPure Donkey anti-rabbit IgG (Jackson ImmunoResearch Laboratory
26 Inc.), dilute 1:500 for 1 hour. Nuclei were stained with 4, 6-diamidino-2-phenylindole (DAPI)
27 (Santa Cruz Biotechnology sc3598). Images were captured using a Quorum spinning disk
28 microscope [Leica DMIRE2 inverted fluorescence microscope equipped with a Hamamatsu
29 back-thinned electron multiplying chargecoupled device camera, spinning disc head, and
30

1
2
3 Volocty 5 software (Improvision)]. Images were imported into Adobe Photoshop and assembled
4 in Adobe Illustrator software. To quantify the percentage of cells with apoB-GFP-LC3 puncta, at
5 least 200 cells per condition were counted in randomly selected fields. In all cases, only those
6 cells with 4 or more prominent puncta of apoB-GFP-LC3 were scored positively.
7
8

9
10 **Statistic analysis.** At least 3 independent experiments were performed for each graph, unless
11 otherwise indicated. The mean \pm SEM is shown in figures. All statistical calculations were
12 completed using GraphPad PRISM software (v5). For grouped analyses, a two way ANOVA
13 was used followed by a Bonferroni post-hoc test. To compared control to different treatments a
14 one way ANOVA was applied followed by a Dunnett's Multiple Comparison Test.. Probability
15 values of less than 0.05 were considered to be statistically significant.
16
17
18
19
20
21
22
23
24
25
26
27
28
29
30
31
32
33
34
35
36
37
38
39
40
41
42
43
44
45
46
47
48
49
50
51
52
53
54
55
56
57
58
59
60

Results

Accumulation of apoB in autophagosomes following treatment of McA-RH7777 cells with glucosamine and tunicamycin. As a first approach to gain insight into the role of autophagy under ER stress conditions, we examined the co-localization of apoB with LC3 (the microtubule associated protein 1 light chain 3), an autophagosome marker. Co-localization of apoB with GFP-LC3 was barely detectable (Figure 1A panels a-c) under untreated conditions in McA-RH7777 cells transiently expressing GFP-conjugated LC3 (GFP-LC3) for 24 hours. However, the co-localization of apoB with GFP-LC3, referred to as apoB-GFP-LC3 puncta, was markedly enhanced following 4 mM glucosamine treatment for 4 hours (Figure 1A panel d-f). Increasing the glucosamine concentration to 16 mM led to high levels of apoB-GFP-LC3 puncta concentrated in a juxtanuclear localization, and in the distal area near the plasma membrane (Figure 1A panels g-i). As depicted in Figure 1B, the density of apoB-GFP-LC3 puncta positive cells as well as the number of apoB-GFP-LC3 puncta in each positive cell increased with rising concentrations of glucosamine (0-16 mM) ($*p<0.05$). Concomitantly, increased apoB-GFP-LC3 puncta were correlated positively with the degradation of newly-synthesized apoB100 in a glucosamine dose dependent manner ($*p<0.05$) (Figure 1C). Moreover, as shown in Figure 1 E, under the basal (Figure 1D, panel c), and tunicamycin (Figure 1D, panel f) or glucosamine (Figure 1D, panel i) treated conditions, the apoB-GFP-LC3 puncta positive cells, and number of apoB-GFP-LC3 puncta was substantially increased by a longer GFP-LC3 expression time (48 hours). Under our experimental conditions, apoB autophagy appeared to account for 15-20% of total apoB loss during glucosamine induced ER stress.

Links between ER stress and apoB autophagy. We next sought to further investigate links between the induction of ER stress and the autophagic degradation of apoB. Experiments were performed in McA-RH7777 cells treated with tunicamycin (5 µg/ml) or glucosamine (5 mM) for 4 hours in the presence or absence of 4-Phenyl butyric acid (PBA, 1 mM), a chemical inhibitor of ER stress (26). Treatment with tunicamycin or glucosamine resulted in increased apoB-GFP-LC3 puncta positive cells and a higher number of apoB-GFP-LC3 puncta in each cell (Figure 2A, panels f and i; and analysis of data shown in Figure 2C; (different letters indicate significance, $p<0.05$), as well as elevated levels of GFP-LC3-II conversion, an autophagosome membrane associated lipidated protein conjugated to GFP (Figure 2D and G; (different letters indicate significance, $p<0.05$)). PBA treatment significantly reduced ER stress-induced formation of apoB-GFP-LC3 positive cells and number of apoB-GFP-LC3 puncta (Figure 2B, and analysis data shown in Figure 2C; $p<0.05$), and prevented apoB-GFP-LC3-II conversion (Figure 2D and G; $p<0.05$). Furthermore, PBA treatment markedly inhibited ER stress based on reduced cellular levels of GRP78 and phosphorylated eIF-2 α (Figure 2D-F). PBA treatment also prevented the loss of newly-synthesized cellular and secreted apoB-100 (Figure 2H-J) following tunicamycin and glucosamine treatment (different letters indicate significance , $p<0.05$). These results strongly indicate that the induction of ER stress augments autophagic degradation of apoB, while suppression of ER stress blocks apoB autophagy.

Evidence of ER stress induced autophagy in primary rat hepatocytes. We next assessed whether autophagic degradation of apoB also occurs in primary hepatocytes. Primary rat hepatocytes were transiently transfected with GFP-LC3 cDNA for 40 hours, and then treated with tunicamycin (5 µg/ml) or glucosamine (5 mM) for 4 hours in the presence or absence of PBA (1 mM). Treatment with tunicamycin or glucosamine resulted in substantially increased co-

1
2
3 localization of apoB with GFP-LC3 and increased number of apoB-GFP-LC3 puncta (Figure 3A,
4 panels f and i; analysis of data shown in Figure 3C; * $p<0.05$ vs corresponding control). Increased
5 apoB-GFP-LC3 puncta were observed together with elevated endogenous LC3-II conversion
6 (Figure 3D; * $p<0.05$). Importantly, treatment with tunicamycin and glucosamine also decreased
7 ^{35}S labelled cellular and secreted apoB100 (Figure 3 E and F; (different letters indicate
8 significance , $p<0.05$), but not apoB48 suggesting that ER stress induces autophagy of apoB100
9 in primary rat hepatocytes. Importantly, PBA treatment inhibited co-localization of apoB with
10 GFP-LC3 (Figure 3B, panels f and i; analysis of data shown in Figure 3C), blocked the
11 endogenous LC3-II conversion (Figure 3D, (different letters indicate significance , $p<0.05$), and
12 led to a significantly increased recovery of ^{35}S labelled cellular or secreted apoB100 (Figure 3 E
13 and F;(different letters indicate significance , $p<0.05$), suggesting that blocking ER stress
14 prevents apoB autophagy. Interestingly, PBA was also found to significantly block co-
15 localization of apoB with GFP-LC3 in primary rat hepatocytes under basal conditions (Figure 3C;
16 top panel, * $p<0.05$ vs corresponding control). However, under basal conditions, PBA did not
17 significantly alter the number of apoB-GFL-LC3 puncta in positive cells (Figure 3C; bottom
18 panel), or endogenous LC3-II conversion (Figure 3D).

19
20
21
22
23
24
25
26
27
28
29
30
31
32
33
34
35
36
37
38
39
40
41
42 ***ER stress-induced autophagy of apoB-GFP-LC3 is decreased by the autophagy inhibitor 3-***
43 ***MA and enhanced by the lysosomal protease inhibitor E64d.*** In order to explore the
44 mechanisms by which apoB is degraded by autophagy, primary rat hepatocytes were transiently
45 transfected with GFP-LC3 cDNA for 44 hours then treated with tunicamycin (5 $\mu\text{g}/\text{ml}$) or
46 glucosamine (5 mM) in the presence or absence of 3-methyadenine (5 mM), an autophagy
47 inhibitor(15), or E64d (5 $\mu\text{g}/\text{ml}$), a lysosome protease inhibitor (27) for 4 hours. Chemical
48 induction of ER stress significantly increased apoB-GFP-LC3 positive cells and the number of
49
50
51
52
53
54
55
56
57
58
59
60

apoB-GFP-LC3 puncta (Figure 4A; panels f and i; analysis of data shown in Figure 4D and E; * $p<0.05$ vs corresponding control). Endogenous LC3-II conversion (Figure 4F; * $p<0.05$ vs corresponding control) was significantly increased as compared to basal controls. The addition of 3-MA significantly decreased the number of apoB-GFP-LC3 positive cells and the number of apoB-GFP-LC3 puncta (Figure 4B panels c, f, and i; and analysis of data shown in Figure 4D and E, * $p<0.05$ vs corresponding control), and endogenous LC3-II conversion (Figure 4F; $p<0.05$) under basal and ER stress conditions. By contrast, addition of the lysosomal protease inhibitor E64d, markedly increased the number of apoB-GFP-LC3 positive cells and the number of apoB-GFP-LC3 puncta (Figure 4C panels c, f and i; analysis of data shown in Figure 4D and E, $p<0.05$), as well as endogenous LC3-II conversion (Figure 4F; * $p<0.05$ vs corresponding control). Taken together, these data further support the induction of apoB autophagy in a process that involves the formation of autophagosomes and accumulation in lysosomes for eventual proteolysis.

ER stress-induced apoB autophagy in primary hepatocytes and established hepatocyte cell lines. To better understand the extent of apoB autophagy in various cell lines and primary hepatocytes, we conducted further experiments in primary hamster hepatocytes (which similar to human hepatocytes secrete only apoB100), as well as the cultured human hepatocyte model, HepG2, a well-characterized model for studies of apoB degradation. As demonstrated in Figure 5A, induction of ER stress following treatment with tunicamycin or glucosamine markedly increased apoB-GFP-LC3 positive cells and the number of apoB-GFP-LC3 puncta in primary hamster hepatocytes (Figure 5B, * $p<0.05$ vs corresponding control). In contrast, this apoB-autophagic degradation was not observed in HepG2 cells under ER stress conditions (Figure 5C). Co-localization of apoB with GFP-LC3 was only observed once proteasomal degradation was

1
2
3 blocked with ALLN and the medium was supplemented with oleic acid (Figure 5D panel i;
4 analysis of data shown in Figure 5E) suggesting that degradation of apoB towards proteasomal or
5 autophagic pathway may be metabolically regulated. More data on apoB-GFP-LC3 puncta in
6 various cell lines in ER stressed conditions is given in supplemental data 2.
7
8

9
10 ***ER stress induction of apoB autophagy is linked to the activation of PERK and IRE1.*** To
11 examine underlying mechanisms, mRNA levels of key molecules in ER stress pathways were
12 determined following 0, 2, 4, and 16 hours of treatment with glucosamine (5 mM) or
13 tunicamycin (5 µg/ml) in the presence or absence of PBA (1 mM). As shown in Figure 6A and B,
14 the mRNA levels of GRP78, PERK and ratio of spliced/unspliced form of Xbp-1 were
15 significantly increased by 1.7 fold (* $p< 0.05$), 1.45 fold (* $p< 0.05$), and 4.23 fold (* $p<0.05$),
16 respectively, following glucosamine treatment. ATF6 mRNA level remained unchanged. PBA
17 treatment markedly inhibited increases in mRNA levels of GRP78, PERK and ratio of
18 spliced/unspliced form of Xbp-1($p<0.05$), suggesting that under our experimental conditions,
19 PERK and IRE1, but not ATF6 signaling may be linked to apoB-autophagic degradation. Similar
20 results were observed in cells treated with tunicamycin (Figure 6 C and D).
21
22

23 ***ER stress induces apoB autophagy via a PERK-dependent mechanism.*** To investigate the role
24 that PERK activation may play in ER stress-induced apoB autophagic degradation, we co-
25 transfected McA-RH7777 cells with GFP-LC3 cDNA and wild-type (WT) PERK cDNA, or
26 kinase inactive (K618A) mutant (M) PERK cDNA, or control (mock), and examined the co-
27 localization of apoB with GFP-LC3 following tunicamycin or glucosamine treatment. Under
28 basal conditions (in the absence of ER stress inducing agents), transfection with PERK WT
29 cDNA led to a significantly increased number of apoB-GFP-LC3 positive cells and the number
30 of apoB-GFP-LC3 puncta (Figure 7A panels c and f; analysis of data shown in Figure 7D and E;
31
32
33
34
35
36
37
38
39
40
41
42
43
44
45
46
47
48
49
50
51
52
53
54
55
56
57
58
59
60

* $p<0.05$ vs mock), as well as elevated GFP-LC3-II conversion (Figure 7F; * $p<0.05$ vs mock), compared with mock transfected cells. In contrast, transfection with the kinase inactive mutant PERK (M PERK) had an opposite effect (Figure 7A; panels c and i; analysis of data shown in Figure 7D-F, * $p<0.05$ vs mock). Similar effects were observed following the induction of ER stress induced by tunicamycin or glucosamine. As demonstrated in Figure 7B and C, in the presence of either tunicamycin or glucosamine, overexpression of wild-type PERK led to increases in apoB-GFP-LC3 positive cells and the number of apoB-GFP-LC3 puncta (analysis of data shown in Fig. D and E; * $p<0.05$ vs mock), and higher GFP-LC3-II conversion (analysis of data shown in Figure 7 F; * $p<0.05$ vs mock) when compared to mock-transfected cells. By contrast, transfection with the kinase inactive mutant PERK significantly blocked ER stress-induced apoB autophagy (analysis of data shown in Figure 7 D-F; * $p<0.05$ vs mock). Taken together, these data suggest that ER stress-induced apoB-autophagic degradation is PERK signalling dependent.

Discussion

In response to ER stress, mammalian cells initially react by attenuating protein synthesis which prevents further accumulation of unfolded proteins in the ER (28). This response is followed by transcriptional induction of ER chaperone genes to increase protein folding capacity and transcriptional induction of ERAD component genes to increase ERAD. The activation of autophagic degradation and induction of apoptosis are late defensive and surveillance systems to safely dispose of organelles and cells injured by ER stress to ensure the survival of the organism (29). Numerous studies have now demonstrated a direct link between induction of ER stress and autophagy (15) and have proposed this pathway as an essential component of the unfolded protein response (30).

Among mammalian proteins, apoB is particularly prone to misfolding under ER stress conditions due to its large size and its requirement for lipid binding to facilitate folding and lipoprotein assembly. Interest in ER stress-induced apoB degradation has also arisen owing to the important role of apoB in cardiovascular disease and recent data implicating apoB as a potential factor linking hepatic ER stress and insulin resistance (31). Early work in our laboratory demonstrated that apoB protein synthesis was attenuated (22), and proteasomal degradation was increased following glucosamine induced ER stress (17). These studies also suggested the involvement of a post-translational degradative mechanism responsible for ER stress related late stage degradation of misfolded apoB (20). Evidence obtained in the present study suggests that ER stress induced autophagy may be responsible for the post-translational loss of misfolded apoB. Following the induction of ER-stress by glucosamine in McA-RH7777 cells, there was a marked increase in co-localization of apoB with the autophagic marker, GFP-LC3, concomitant with a decrease in newly-synthesized apoB100, and elevated mRNA levels of

1
2
3 PERK and spliced Xbp-1, and phospho-eIF2 α and GRP78. 4-Phenyl butyric acid (PBA), a
4 chemical ER-stress inhibitor could not only prevent ER-stress induced reduction of newly-
5 synthesized apoB100, but also inhibited the number of apoB-GFP-LC3 puncta and the
6 conversion of GFP-LC3-II, an autophagosome marker in McA-RH7777. These data clearly
7 suggest that ER stress induced apoB degradation is associated with autophagy.
8
9
10
11
12
13
14

15 To assess whether autophagy is a common mechanism for ER stress-induced apoB
16 turnover in hepatic cells, we monitored this process in two liver cell lines, namely, HepG2 and
17 McA-RH7777 rat hepatoma cells and primary hepatocytes isolated from rats and hamsters.
18 ApoB-autophagic degradation was not detected in HepG2 cells following the induction of ER
19 stress, unless proteasomal degradation was inhibited by ALLN and cells were supplemented with
20 oleic acid. This was not unexpected since we previously reported that the predominant
21 mechanism of apoB degradation following ER stress in HepG2 cells was proteasomal in nature
22 (17). Our current data appears to suggest that blocking proteasomal degradation in ER stressed
23 HepG2 cells leads to the activation of apoB autophagy, which may act to clear apoB aggregates
24 accumulating in the ER in the absence of proteasome activity. These data also suggest that
25 proteasomal and autophagic degradative pathways may in fact be co-ordinately regulated.
26 Proteasomal degradation is perhaps an early quality control system, whereas, apoB-autophagic
27 degradation may be a late quality control mechanism. It is likely that newly-synthesized apoB
28 molecules that escape the early-stage proteasomal degradation may become substrates for
29 autophagy if not properly lipidated and removed from the secretory pathway. This hypothesis is
30 supported by a recent study by Zhong et al. who showed that expression of A31P, an apoB
31 mutant, leads to rapid proteasomal degradation, but a significant proportion of A31P escapes the
32
33
34
35
36
37
38
39
40
41
42
43
44
45
46
47
48
49
50
51
52
53
54
55
56
57
58
59
60

1
2
3 ER quality control and is present in the Golgi compartment. However, post-ER degradation of
4 A31P was found to occur via autophagy (14).
5
6

7 Importantly, we have presented evidence of apoB autophagy in both primary rat and
8 primary hamster hepatocytes under basal and ER stress-induced conditions. ApoB-GFP-LC3
9 puncta was clearly detectable in both rat and hamster primary hepatocytes under basal conditions,
10 and was considerably enhanced following the induction of ER stress. These data suggest that
11 apoB autophagy is likely an important mechanism of apoB turnover in primary hepatocytes and
12 is active in unstressed and stressed conditions. Interestingly, apoB autophagy was robustly
13 inhibited when cells were treated with PBA, a chemical agent that facilitates protein folding in
14 the cell. Fisher and co-workers were first to demonstrate DHA-induced apoB-autophagic
15 degradation in McA-RH7777 cells due to accumulation of lipid peroxides in or after the Golgi
16 apparatus. ApoB was shown to undergo oxidative damage, to form aggregates, and to
17 subsequently be diverted out of the secretory pathway by autophagosomes for delivery to
18 lysosomes for destruction (13). In the present study, while PBA could prevent ER stress-induced
19 apoB-autophagic degradation, it was unable to inhibit DHA-induced or ALLN-induced apoB
20 autophagy in rat primary hepatocytes (see supplemental data 3), suggesting that the mechanisms
21 mediating apoB-autophagic degradation under ER stress may be different from that induced by
22 DHA or ALLN.
23
24

25 Although a large body of evidence suggests that ER stress regulates autophagic
26 degradation (30), the underlying mechanisms remain to be elucidated. Three pathways (PERK,
27 ATF6, and IRE1 pathways) regulate the mammalian ER stress response (29). PERK, a
28 transmembrane kinase, phosphorylates eIF2 α to attenuate translation, and to up-regulate
29 expression of ATF4, leading to enhanced transcription of target genes such as CHOP. ATF6, a
30
31
32
33
34
35
36
37
38
39
40
41
42
43
44
45
46
47
48
49
50
51
52
53
54
55
56
57
58
59
60

transmembrane transcription factor, is translocated to the Golgi apparatus and cleaved by proteases such as S1P and S2P, leading to enhanced transcription of ER chaperone genes. IRE1, a transmembrane RNase, splices Xbp1 pre-mRNA, and pXbp1(S) translated from mature Xbp1 mRNA activates transcription of ERAD component genes. In the present study, we found that the ATF6 pathway is inactive upon acute ER stress (induced by tunicamycin or glucosamine) perhaps since ATF6 has been suggested to regulate chronic ER stress (32). By contrast, PERK activation appeared to be critical to ER stress-induced activation of apoB-autophagic degradation. Our observations are consistent with a previous report that PERK/eIF2 α phosphorylation plays a critical role in mediating autophagosome associated LC3-II conversion during ER stress induced by polyglutamine 72 repeat (polyQ72) aggregates (33). It remains to be defined whether or not Xbp1 also play a role in apoB-autophagic degradation.

In summary, these data collectively suggest that apoB-autophagic degradation in hepatic cells is largely dependent upon the cell type used and cell culture conditions. This pathway is inactive in HepG2 cells but can be activated if proteasomal degradation is inhibited by ALLN and supplemented with oleate. ApoB-autophagic degradation is however highly active in primary hepatocytes under both normal and ER stress conditions. Ameliorating ER stress with chemical chaperones such as PBA abolishes apoB-autophagic degradation under ER stress conditions. Finally, induction of PERK signalling may be essential to apoB autophagy.

Acknowledgements– We would like to acknowledge Mark Naples and Chris Baker for expert technical assistance with isolation of rat and hamster primary hepatocytes. This work was supported by an operating grant (T-6658) from Heart and Stroke Foundation of Ontario to KA.

Figure legends

Figure 1. Glucosamine induces co-localization of apoB with GFP-LC3 in a dose dependent manner. (A) Glucosamine (GLS) induced co-localization of apoB (b, e, h; red) with GFP-LC3 (a, d, g; green), referred to as apoB-GFP-LC3 puncta (c, f, i; yellow). Confocal microscopy photographs are shown from 3 independent experiments. McA-RH7777 cells were transiently transfected with GFP-LC3 cDNA for 24 hours in the presence of GLS (0 – 16 mM; 4 hours). Scale bar: 7 μ M. (B) Top panel shows percentage of apoB-GFP-LC3 positive cells, and bottom panel shows the number of apoB-GFP-LC3 puncta in positive cells; * $p<0.05$ vs untreated (0 mM GLS). (C) Glucosamine treatment (0–16 mM) of McA-RH7777 cells (4 hours) decreased newly-synthesized apoB100 in a dose dependent manner. The samples were first immunoprecipitated (IP) with anti-apoB antibody followed by a second IP with anti-albumin antibody. Data analysis is shown in the bottom panel; n=4 * $p<0.05$ vs untreated (0 mM GLS). (D) Tunicamycin (TM) and glucosamine (GLS) induced co-localization of apoB (b, c, e; red) with GFP-LC3 (a, d, g; green), apoB-GFP-LC3 puncta (c, f, i; yellow). McA-RH7777 cells were transiently transfected with GFP-LC3 cDNA for 48 hours. Scale bar: 7 μ M. (E) Data analysis is shown from cells transfected with GFP-LC3 cDNA for 24 or 48 hours; n=3, * $p<0.05$ vs corresponding untreated timepoint. .

Figure 2. PBA (4-Phenyl butyric acid) prevents ER stress-induced apoB autophagy in McA-RH7777 cells. (A and B) PBA treatment of McA-RH7777 cells blocks tunicamycin (TM) and glucosamine (GLS) induced co-localization of apoB with GFP-LC3. ApoB is labeled red (b, e, h); and GFP-LC3 is labeled green (a, d, g); apoB-GFP-LC3 puncta are labeled yellow (c, f and i). Scale bar: 7 μ M. (C) Data analysis from (A and B), top panel shows percentage of apoB-GFP-LC3 positive cells, and bottom panel shows the number of apoB-GFP-LC3 puncta in

positive cells; n=3, with different letters indicating significance $p<0.05$. (D) PBA treatment of McA-RH7777 cells blocks tunicamycin (TM) and glucosamine (GLS) induced levels of GRP78, phosphorylation of eIF2 α , and ratio of GFP-LC3-II/GFP-LC3-I conversion. Representative western blots are shown as well as data analysis from three independent experiments (E-G); with different letters indicating significance , $p<0.05$. (H) PBA treatment of McA-RH7777 cells normalizes tunicamycin (TM) and glucosamine (GLS) induced decreases in newly-synthesized apoB100; data analysis is shown in (I and J); n=3, with different letters indicating significance, $p<0.05$.

Figure 3. PBA prevents ER stress induced apoB-autophagy in primary rat hepatocytes. (A and B). Confocal microscopy photographs showing co- localization of apoB (b, e, h, red) with GFP-LC3 (a, d, g, green), and apoB-GFP-LC3 puncta (c, f, i, yellow), in primary rat hepatocytes following treatment with tunicamycin (TM) or glucosamine (GLS). Scale bar: 11 μ M. (C) Data analysis is shown in the top panel showing percentage of apoB-GFP-LC3 positive cells, and the bottom panel shows the number of apoB-GFP-LC3 puncta in positive cells; n= 3, * $p<0.05$ vs corresponding control. PBA also reduced the conversion of endogenous LC3-II/LC3-1 (D), and increased recovery of newly-synthesized apoB100 (E and F), in cells treated with tunicamycin or glucosamine; 3 independent experiments, * $p<0.05$ vs corresponding control.

Figure 4. 3-MA blocks while E64d enhances apoB-GFP-LC3 puncta induced by ER stress. (A-C) Confocal microscopy photographs of primary rat hepatocytes treated with tunicamycin (TM, 5 μ g/ml) or glucosamine (GLS, 5 mM) in the presence of 3-MA (3-methyadenine) (5 mM) or E64d (5 μ g/ml). Co-localization of apoB (b, e, h, red) with GFP-LC3 (a, d, g, green), apoB-GFP-LC3 puncta (c, f, i, yellow). Scale bar: 17 μ M. Data analysis from (A-C) is shown in (D), percentage of apoB-GFP-LC3 positive cells, and (E), the numbers of apoB-GFP-LC3 puncta in

positive cells; 3 independent experiments * $p < 0.05$. 3-MA blocked and E64d increased the conversion of endogenous LC3-II (F) when exposed to tunicamycin or glucosamine treatment, n=3, * $p < 0.05$.

Figure 5. ER stress-induced co-localization of apoB with GFP-LC3 is cell type dependent.

(A) Confocal microscopy photographs showing co-localization of apoB (b, e, h, red) with GFP-LC3 (a, d, g, green), and apoB-GFP-LC3 puncta (c, f, i, yellow), in primary hamster hepatocytes following treatment with tunicamycin (TM) or glucosamine (GLS). Scale bar: 14 μM . (B) Data analysis from (A), showing percentage of apoB-GFP-LC3 positive cells, and the number of apoB-GFP-LC3 puncta in positive cells; 3 independent experiments, * $p < 0.05$ vs corresponding control. (C and D) The co-localization of apoB (red) with GFP-LC3 (green) in HepG2 cells in the presence of ALLN (20 $\mu\text{g/ml}$) plus oleic acid (0.4 mM). Scale bar: 7 μM . (E) Data analysis from (D); 3 independent experiments, * $p < 0.05$ vs oleate alone.

Figure 6. ER stress induction is linked to the activation of PERK and IRE1. mRNA levels of GRP78, PERK, and Xbp1 (spliced) in McA-RH77777 cells treated with glucosamine (A and B), or tunicamycin (C and D). (A) The blots of RT-PCR products in glucosamine treated cells (0, 2, 4, and 16 hours; 5 mM) in the presence or absence of PBA (1 mM) are shown. (B) Data analysis from (A); 3 independent experiments. * $p < 0.05$ vs 0h. (C) Shown are the blots of RT-PCR products from McA-RH77777 cells treated with tunicamycin (0, 2, 4, and 16 hours; 5 $\mu\text{g/ml}$) in the presence or absence of PBA (1 mM). (D) Data analysis were from (C); 3 independent experiments. * $p < 0.05$ vs 0h

Figure 7. ER stress-induced apoB autophagy is PERK signaling dependent. McA-RH7777 cells were transiently transfected with GFP-LC3 cDNA alone or with wild type PERK (WT-PERK) or kinase inactive (K618A) PERK (M-PERK) for 48h in the absence (A) or presence of

tunicamycin (TM) (B) or glucosamine (GLS)(C). (A-C) Confocal microscopy photographs showing co-localization of apoB (b, e, h, red) with GFP-LC3 (a,d,g, green), and apoB-GFP-LC3 puncta (c, f, i, yellow). Scale bar: 17 μ M. (D and E) Data analysis from (A-C); * $p<0.05$ vs corresponding mock treatment. (F) Western blots showing the levels of GFP-LC3-I and GFP-LC3-II; (top panel), β -actin as a protein loading control; and the fold ratio of GFP-LC3-II/ GFP-LC3-I; (bottom panel); n=3, * $p<0.05$ vs corresponding mock treatment.

For Peer Review

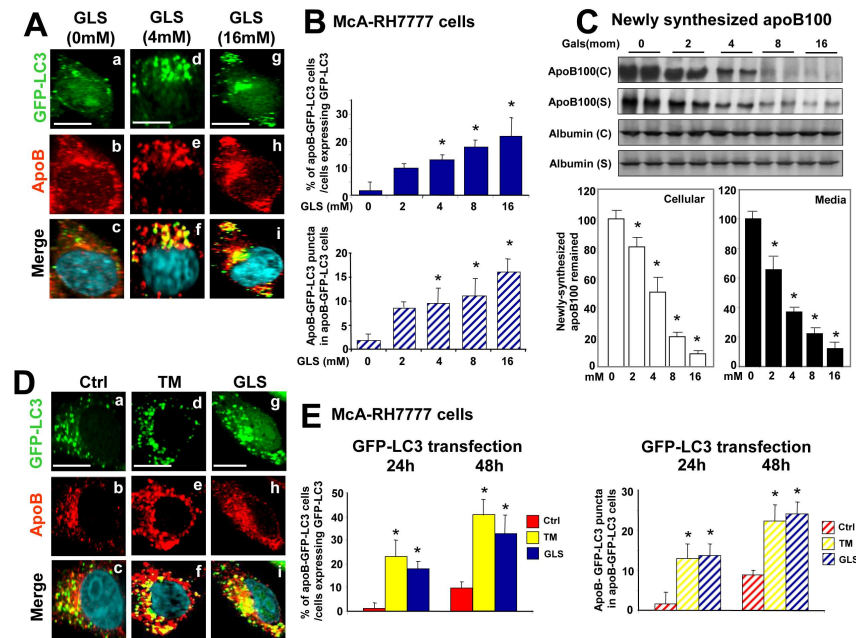
Reference List

- 1
- 2
- 3
- 4
- 5
- 6
- 7
- 8 1. Rutledge AC, Su Q, Adeli K. Apolipoprotein B100 biogenesis: a complex array of
9 intracellular mechanisms regulating folding, stability, and lipoprotein assembly. *Biochem
10 Cell Biol* 2010; 88(2):251-267.
- 11
- 12 2. Sundaram M, Yao Z. Recent progress in understanding protein and lipid factors affecting
13 hepatic VLDL assembly and secretion. *Nutr Metab (Lond)* 2010; 7:35.
- 14
- 15 3. Liao W, Yeung SC, Chan L. Proteasome-mediated degradation of apolipoprotein B targets
16 both nascent peptides cotranslationally before translocation and full-length apolipoprotein
17 B after translocation into the endoplasmic reticulum. *J Biol Chem* 1998; 273(42):27225-
18 27230.
- 19
- 20 4. Fisher EA, Zhou M, Mitchell DM, Wu X, Omura S, Wang H et al. The degradation of
21 apolipoprotein B100 is mediated by the ubiquitin-proteasome pathway and involves heat
22 shock protein 70. *J Biol Chem* 1997; 272(33):20427-20434.
- 23
- 24 5. Zhou M, Fisher EA, Ginsberg HN. Regulated Co-translational ubiquitination of
25 apolipoprotein B100. A new paradigm for proteasomal degradation of a secretory protein. *J
26 Biol Chem* 1998; 273(38):24649-24653.
- 27
- 28 6. Taghibiglou C, Rudy D, Van Iderstine SC, Aiton A, Cavallo D, Cheung R et al.
29 Intracellular mechanisms regulating apoB-containing lipoprotein assembly and secretion in
30 primary hamster hepatocytes. *J Lipid Res* 2000; 41(4):499-513.
- 31
- 32 7. Adeli K. Regulated intracellular degradation of apolipoprotein B in semipermeable HepG2
33 cells. *J Biol Chem* 1994; 269(12):9166-9175.
- 34
- 35 8. Cavallo D, Rudy D, Mohammadi A, Macri J, Adeli K. Studies on degradative mechanisms
36 mediating post-translational fragmentation of apolipoprotein B and the generation of the
37 70-kDa fragment. *J Biol Chem* 1999; 274(33):23135-23143.
- 38
- 39 9. Du EZ, Kurth J, Wang SL, Humiston P, Davis RA. Proteolysis-coupled secretion of the N
40 terminus of apolipoprotein B. Characterization of a transient, translocation arrested
41 intermediate. *J Biol Chem* 1994; 269(39):24169-24176.
- 42
- 43 10. Twisk J, Gillian-Daniel DL, Tebon A, Wang L, Barrett PH, Attie AD. The role of the LDL
44 receptor in apolipoprotein B secretion. *J Clin Invest* 2000; 105(4):521-532.
- 45
- 46 11. Luo Y, Warren L, Xia D, Jensen H, Sand T, Petras S et al. Function and distribution of
47 circulating human PCSK9 expressed extrahepatically in transgenic mice. *J Lipid Res* 2009;
48 50(8):1581-1588.
- 49
- 50
- 51
- 52
- 53
- 54
- 55
- 56
- 57
- 58
- 59
- 60

- 1
2
3 12. Ohsaki Y, Cheng J, Fujita A, Tokumoto T, Fujimoto T. Cytoplasmic lipid droplets are sites
4 of convergence of proteasomal and autophagic degradation of apolipoprotein B. *Mol Biol*
5 *Cell* 2006; 17(6):2674-2683.
6
7 13. Pan M, Maitin V, Parathath S, Andreo U, Lin SX, St Germain C et al. Presecretory
8 oxidation, aggregation, and autophagic destruction of apoprotein-B: a pathway for late-
9 stage quality control. *Proc Natl Acad Sci U S A* 2008; 105(15):5862-5867.
10
11 14. Zhong S, Magnolo AL, Sundaram M, Zhou H, Yao EF, Di Leo E et al. Nonsynonymous
12 mutations within APOB in human familial hypobetalipoproteinemia: evidence for feedback
13 inhibition of lipogenesis and postendoplasmic reticulum degradation of apolipoprotein B. *J*
14 *Biol Chem* 2010; 285(9):6453-6464.
15
16 15. He C, Klionsky DJ. Regulation mechanisms and signaling pathways of autophagy. *Annu*
17 *Rev Genet* 2009; 43:67-93.
18
19 16. Ozcan U, Cao Q, Yilmaz E, Lee AH, Iwakoshi NN, Ozdelen E et al. Endoplasmic
20 reticulum stress links obesity, insulin action, and type 2 diabetes. *Science* 2004;
21 306(5695):457-461.
22
23 17. Qiu W, Kohen-Avramoglu R, Mhapsekar S, Tsai J, Austin RC, Adeli K. Glucosamine-
24 induced endoplasmic reticulum stress promotes ApoB100 degradation: evidence for Grp78-
25 mediated targeting to proteasomal degradation. *Arterioscler Thromb Vasc Biol* 2005;
26 25(3):571-577.
27
28 18. Ota T, Gayet C, Ginsberg HN. Inhibition of apolipoprotein B100 secretion by lipid-induced
29 hepatic endoplasmic reticulum stress in rodents. *J Clin Invest* 2008; 118(1):316-332.
30
31
32 19. Li J, Ni M, Lee B, Barron E, Hinton DR, Lee AS. The unfolded protein response regulator
33 GRP78/BiP is required for endoplasmic reticulum integrity and stress-induced autophagy
34 in mammalian cells. *Cell Death Differ* 2008; 15(9):1460-1471.
35
36 20. Qiu W, Avramoglu RK, Rutledge AC, Tsai J, Adeli K. Mechanisms of glucosamine-
37 induced suppression of the hepatic assembly and secretion of apolipoprotein B-100-
38 containing lipoproteins. *J Lipid Res* 2006; 47(8):1749-1761.
39
40 21. Huang J, Canadien V, Lam GY, Steinberg BE, Dinauer MC, Magalhaes MA et al.
41 Activation of antibacterial autophagy by NADPH oxidases. *Proc Natl Acad Sci U S A* 2009;
42 106(15):6226-6231.
43
44 22. Qiu W, Su Q, Rutledge AC, Zhang J, Adeli K. Glucosamine-induced endoplasmic
45 reticulum stress attenuates apolipoprotein B100 synthesis via PERK signaling. *J Lipid Res*
46 2009; 50(9):1814-1823.
47
48 23. Qiu W, Federico L, Naples M, Avramoglu RK, Meshkani R, Zhang J et al. Phosphatase
49 and tensin homolog (PTEN) regulates hepatic lipogenesis, microsomal triglyceride transfer
50 protein, and the secretion of apolipoprotein B-containing lipoproteins. *Hepatology* 2008;
51 48(6):1799-1809.
52
53
54
55
56
57
58
59
60

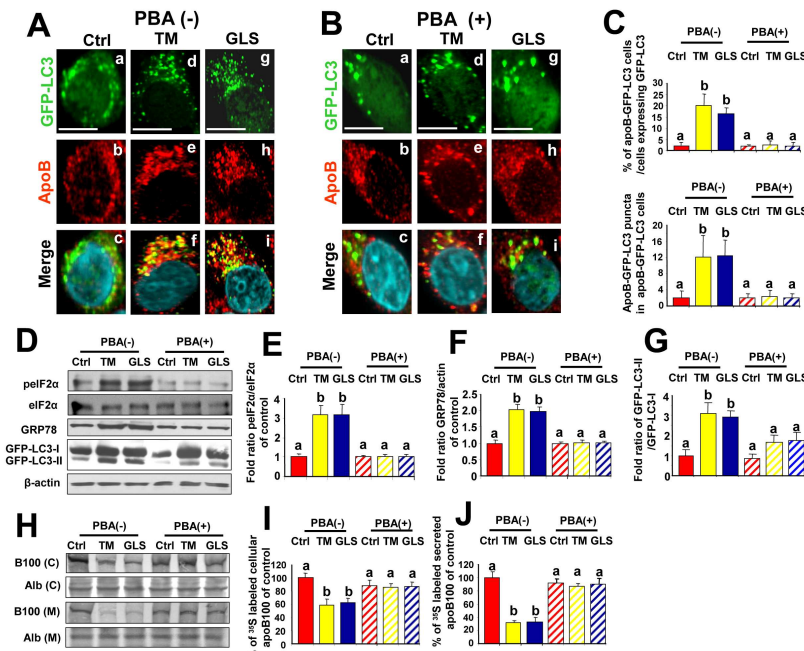
- 1
2
3 24. Qiu W, Kohen-Avramoglu R, Rashid-Kolvear F, Au CS, Chong TM, Lewis GF et al.
4 Overexpression of the endoplasmic reticulum 60 protein ER-60 downregulates apoB100
5 secretion by inducing its intracellular degradation via a nonproteasomal pathway: evidence
6 for an ER-60-mediated and pCMB-sensitive intracellular degradative pathway.
7 Biochemistry 2004; 43(16):4819-4831.
8
9
- 10 25. Qiu W, Avramoglu RK, Dube N, Chong TM, Naples M, Au C et al. Hepatic PTP-1B
11 expression regulates the assembly and secretion of apolipoprotein B-containing
12 lipoproteins: evidence from protein tyrosine phosphatase-1B overexpression, knockout, and
13 RNAi studies. Diabetes 2004; 53(12):3057-3066.
14
15
- 16 26. Ozcan U, Yilmaz E, Ozcan L, Furuhashi M, Vaillancourt E, Smith RO et al. Chemical
17 chaperones reduce ER stress and restore glucose homeostasis in a mouse model of type 2
18 diabetes. Science 2006; 313(5790):1137-1140.
19
20
- 21 27. Tanida I, Minematsu-Ikeguchi N, Ueno T, Kominami E. Lysosomal turnover, but not a
22 cellular level, of endogenous LC3 is a marker for autophagy. Autophagy 2005; 1(2):84-91.
23
24 28. Mori K. Signalling pathways in the unfolded protein response: development from yeast to
25 mammals. J Biochem 2009; 146(6):743-750.
26
27
- 28 29. Yoshida H. ER stress and diseases. FEBS J 2007; 274(3):630-658.
29
30 30. Yorimitsu T, Nair U, Yang Z, Klionsky DJ. Endoplasmic reticulum stress triggers
31 autophagy. J Biol Chem 2006; 281(40):30299-30304.
32
33 31. Su Q, Tsai J, Xu E, Qiu W, Bereczki E, Santha M et al. Apolipoprotein B100 acts as a
34 molecular link between lipid-induced endoplasmic reticulum stress and hepatic insulin
35 resistance. Hepatology 2009; 50(1):77-84.
36
37 32. Wu J, Rutkowski DT, Dubois M, Swathirajan J, Saunders T, Wang J et al. ATF6alpha
38 optimizes long-term endoplasmic reticulum function to protect cells from chronic stress.
39 Dev Cell 2007; 13(3):351-364.
40
41
- 42 33. Kuroku Y, Fujita E, Tanida I, Ueno T, Isoai A, Kumagai H et al. ER stress
43 (PERK/eIF2alpha phosphorylation) mediates the polyglutamine-induced LC3 conversion,
44 an essential step for autophagy formation. Cell Death Differ 2007; 14(2):230-239.
45
46
47
48
49
50
51
52
53
54
55
56
57
58
59
60

Figure 1



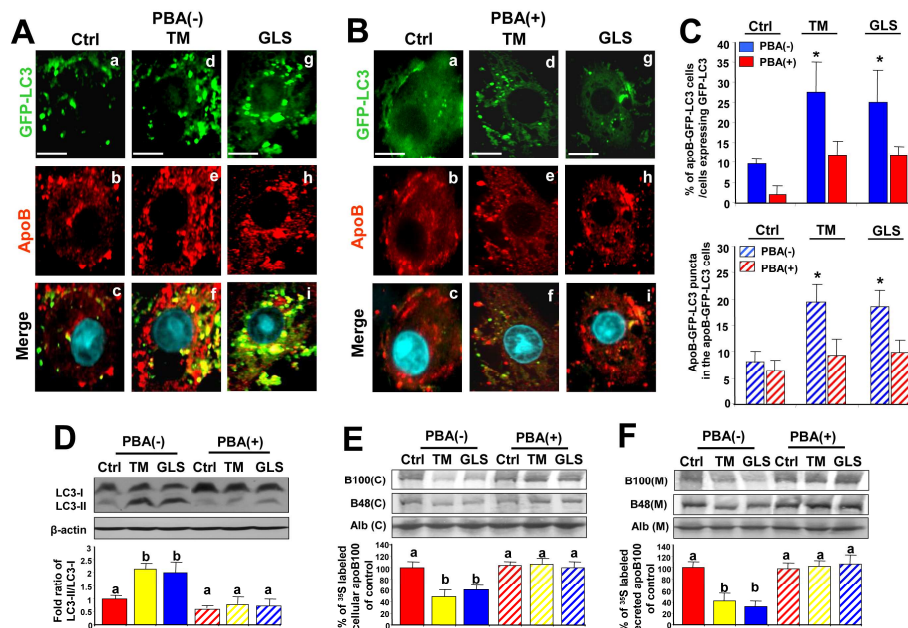
255x190mm (300 x 300 DPI)

Figure 2



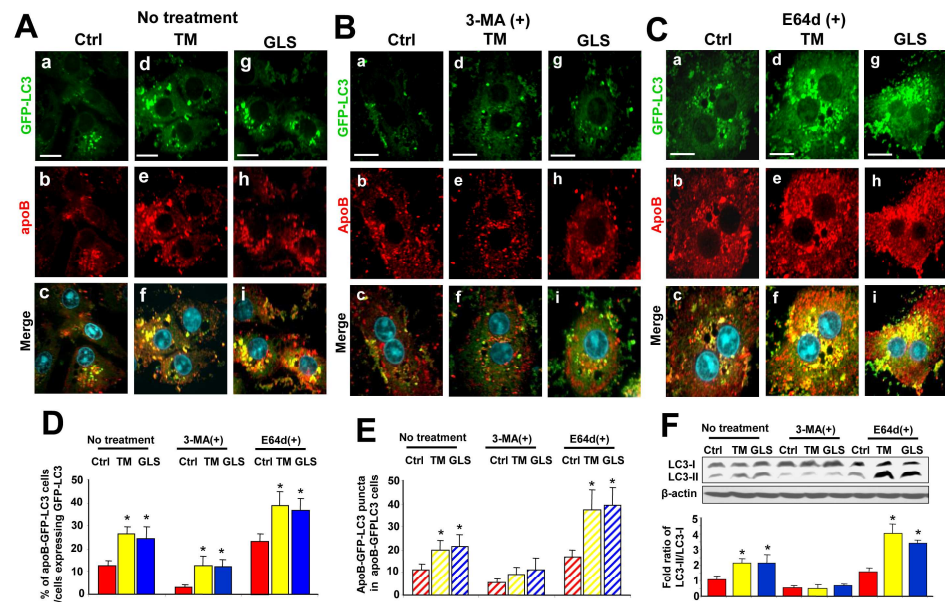
256x190mm (300 x 300 DPI)

Figure 3



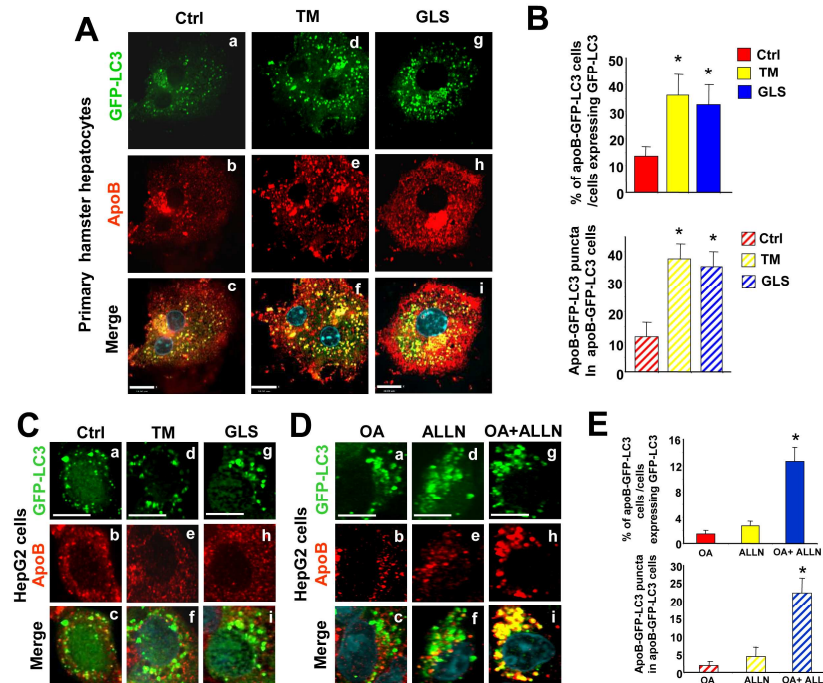
255x190mm (300 x 300 DPI)

Figure 4



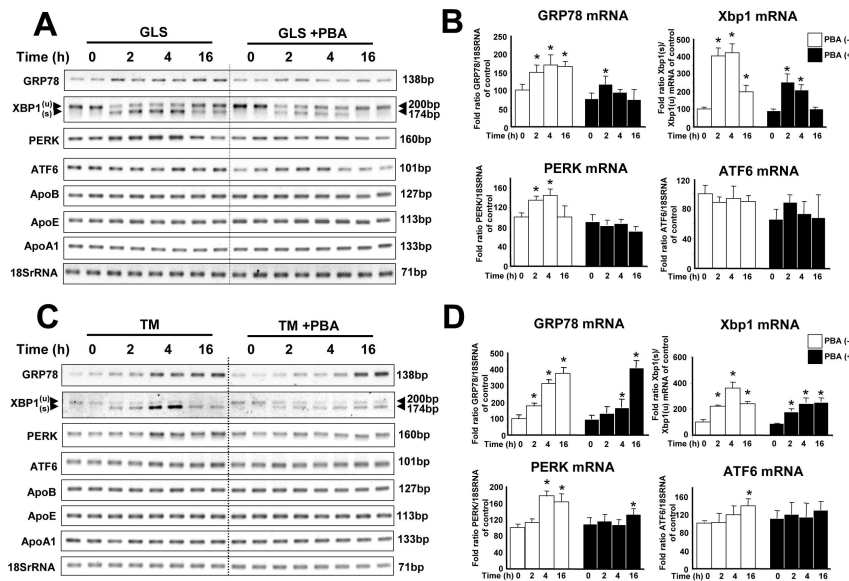
259x190mm (300 x 300 DPI)

Figure 5



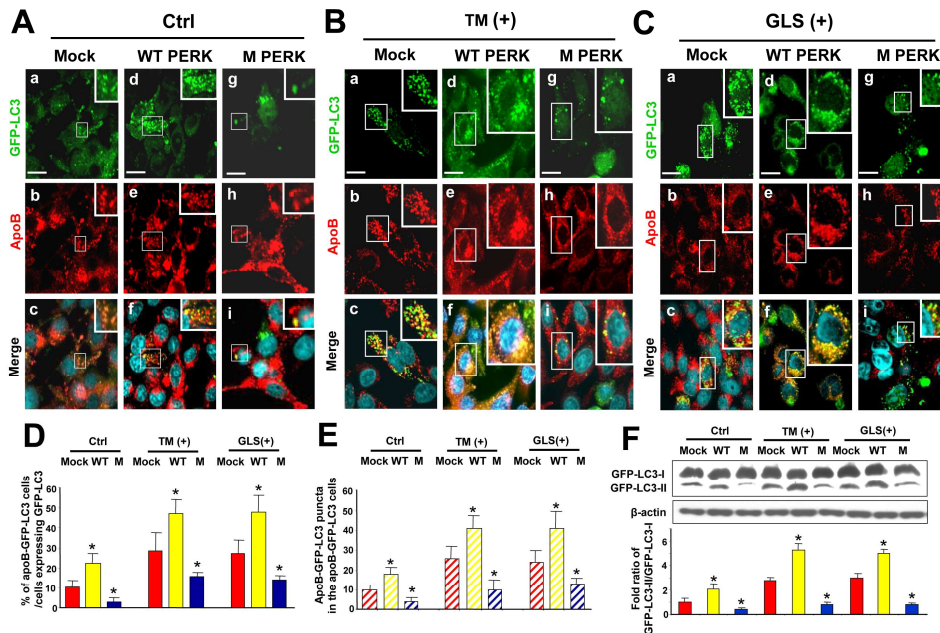
255x190mm (300 x 300 DPI)

Figure 6



256x190mm (300 x 300 DPI)

Figure 7



260x190mm (300 x 300 DPI)

1
2
3
4
5
6
7
8
9

Supplemental data 1

10
11
**Table 1. cDNA sequence of primers used in RT-PCR for detection of
apoB, apoE, apoA1, GRP78, Xbp1, PERK and ATF6 mRNA levels.**

Primers for Rat				
	Gene Bank # & Name		5' → 3'	Product Size (bp)
Apob	NM_019287 Apob	F	TCGTGTGATGGTCTCATC	127
		R	GTCAGGAACTAGATGTTTC	
Apoe	NM_138828 Apoe	F	AAAAAGGACCTGGAGGAACAG	113
		R	CGTAGATCCTCATGTCAGCTC	
Apoa1	NM_012738.1 Apoa1	F	GTGAAGGATTCCCACTGT	133
		R	AACCCAGAGTGTCCCAGTTG	
Grp78	NM_013083 Hsp45	F	AGAGTTCTCAATGCCAAGGAG	138
		R	AGAGGACACACATCAAGCAGAA	
Xbp1(U) Xbp1(S)	NM_001004210.1 Xbp1(U)	F	TCATGGGTTGTGATTGAGA	XBPI(U) 200 XBPI(S) 174
		R	GGAAGATGTTCTGGGAGGT	
Perk	NM_031599.1 Eif2ak3	F	CCAGGCATCGTGAGGTATTT	160
		R	GATCCATCTGCCGATCTTA	
Atf6	NM_001107196.1 Atf6	F	GGAAGTTCCAAGGCTTGTGAC	101
		R	TGGGTGGTAGCTGCTAACAGCA	
18S rRNA	X01117 18S rRNA	F	TAAGTCCCTGCCCTTTGACACA	71
		R	GATCCGAGGGCCTCACTAAAC	

29
30
31
32
33
34 256x190mm (300 x 300 DPI)
35
36
37
38
39
40
41
42
43
44
45
46
47
48
49
50
51
52
53
54
55
56
57
58
59
60

Supplemental data 2

Ratio of the area (pixels) of apoB-GFP-LC3 puncta/ the area (pixels) of apoB in GFP-LC3 transfected cells following treatment of PBA, TM, and GLS

	Treatments	McA	Rat PH	Ham PH	HepG2
PBA (-)	Control	7.4 ± 6.8% (n = 7)	11.3 ± 4.7% (n = 8)	12 ± 6.9% (n = 8)	4.0 ± 3.0% (n = 8)
PBA (-)	Tunicamycin 5µg/ml, 4h	30.0 ± 20.0% (n = 10) *	31.3 ± 16.2% (n = 10) *	28.3 ± 14.1% (n = 10) *	4.1 ± 3.8% (n = 8)
PBA (-)	Glucosamine 5mM , 4h	27.5 ± 16.3% (n = 10) *	32.4 ± 19.5% (n = 10) *	28.1 ± 17.4% (n = 10) *	4.6 ± 4.1% (n = 8)
PBA (+)	Control	8.1 ± 6.5% (n = 9)	5 ± 4.8% (n = 8) †	N/A	N/A
PBA (+)	Tunicamycin 5µg/ml, 4h	7.0 ± 6.7% (n = 10) †	16.9 ± 12.6% (n = 10) †	N/A	N/A
PBA (+)	Glucosamine 5mM , 4h	9.5 ± 4.0% (n = 10) †	18.1 ± 8.8% (n = 10) †	N/A	N/A

McA= McA-RH7777 cells transfected with GFP-LC3 plasmid cDNA for 24h.

Rat PH = rat primary hepatocytes transfected with GFP-LC3 plasmid cDNA for 44h.

Ham PH = hamster primary hepatocytes transfected with GFP-LC3 plasmid cDNA for 44h.

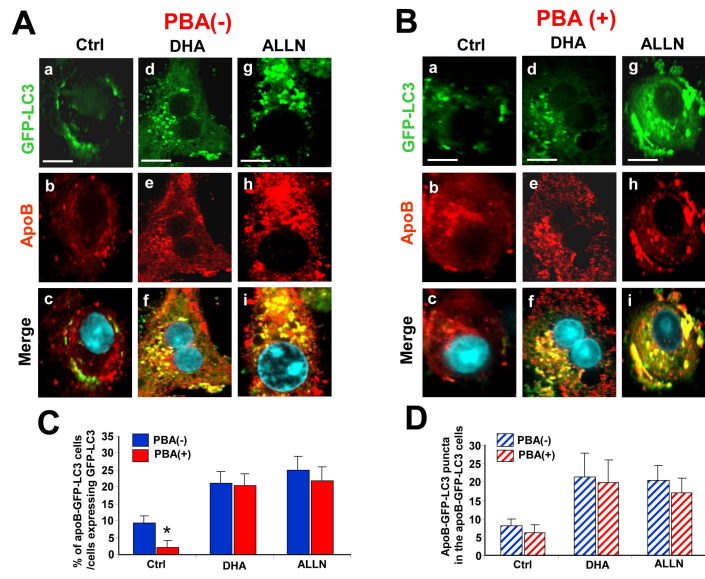
HepG2 cells transfected with GFP-LC3 plasmid cDNA for 44h.

N/A= Not available

*P < 0.05, †P < 0.05.

255x190mm (300 x 300 DPI)

Supplemental data 3



PBA does not prevent DHA or ALLN induced apoB-autophagy in primary rat hepatocytes. Confocal microscopy photographs showing co-localization of apoB (b, e, h, red) with GFP-LC3 (a, d, g, green), and apoB-GFP-LC3 puncta (c, f, i, yellow), in primary rat hepatocytes following treatment with DHA or ALLN. (A) no PBA treatment and (B) treated with PBA. Scale bar: 11 μ M. Data analysis is shown in (C) showing percentage of apoB-GFP-LC3 positive cells, and (D) shows the number of apoB-GFP-LC3 puncta in the positive cells; 3 independent experiments, * $p<0.05$.

256x190mm (300 x 300 DPI)